Molecular regulation of *ZmMs7* required for maize male fertility and development of a dominant male-sterility system in multiple species

Xueli An[a,b,1], Biao Ma[a,b,1], Meijuan Duan[c,1], Zhenying Dong[a,b,1], Ruogu Liu[a,b], Dingyang Yuan[d], Quancan Hou[a,b], Suowei Wu[a,b], Danfeng Zhang[b], Dongcheng Liu[a,b], Dong Yu[d], Yuwen Zhang[a,b], Ke Xie[a,b], Taotao Zhu[a], Ziwen Li[a,b], Simiao Zhang[a], Youhui Tian[a,b], Chang Liu[a], Jinping Li[b], Longping Yuan[d,2], and Xiangyuan Wan[a,b,2]

[a]Zhongzhi International Institute of Agricultural Biosciences, Biology and Agriculture Research Center, University of Science and Technology Beijing, 100024 Beijing, China; [b]Beijing Engineering Laboratory of Main Crop Bio-Tech Breeding, Beijing International Science and Technology Cooperation Base of Bio-Tech Breeding, Beijing Solidwill Sci-Tech Co. Ltd., 100192 Beijing, China; [c]College of Agronomy, Hunan Agricultural University, 410128 Changsha, China; and [d]State Key Laboratory of Hybrid Rice, Hunan Hybrid Rice Research Centre, 410125 Changsha, China

Contributed by Longping Yuan, June 8, 2020 (sent for review May 26, 2020; reviewed by Qian Qian and Feng Tian)

Understanding the molecular basis of male sterility and developing practical male-sterility systems are essential for heterosis utilization and commercial hybrid seed production in crops. Here, we report molecular regulation by genic male-sterility gene *maize male sterility 7* (*ZmMs7*) and its application for developing a dominant male-sterility system in multiple species. *ZmMs7* is specifically expressed in maize anthers, encodes a plant homeodomain (PHD) finger protein that functions as a transcriptional activator, and plays a key role in tapetal development and pollen exine formation. ZmMs7 can interact with maize nuclear factor Y (NF-Y) subunits to form ZmMs7-NF-YA6-YB2-YC9/12/15 protein complexes that activate target genes by directly binding to CCAAT box in their promoter regions. Premature expression of *ZmMs7* in maize by an anther-specific promoter *p5126* results in dominant and complete male sterility but normal vegetative growth and female fertility. Early expression of *ZmMs7* downstream genes induced by prematurely expressed ZmMs7 leads to abnormal tapetal development and pollen exine formation in *p5126-ZmMs7* maize lines. The *p5126-ZmMs7* transgenic rice and *Arabidopsis* plants display similar dominant male sterility. Meanwhile, the *mCherry* gene coupled with *p5126-ZmMs7* facilitates the sorting of dominant sterility seeds based on fluorescent selection. In addition, both the *ms7-6007* recessive male-sterility line and *p5126-ZmMs7M* dominant male-sterility line are highly stable under different genetic germplasms and thus applicable for hybrid maize breeding. Together, our work provides insight into the mechanisms of anther and pollen development and a promising technology for hybrid seed production in crops.

ZmMs7 | PHD finger | protein-protein interaction | dominant male-sterility system

Heterosis is a phenomenon in which heterozygous hybrid progeny are superior to both homozygous parents and can offer 20% to over 50% yield increases in various crops (1). Maize is one of the most successful crops of heterosis utilization. Manual or mechanical detasseling has been widely used for maize hybrid seed production. However, detasseling is not only time consuming, labor intensive, and expensive, but also detrimental to plant growth, and thus reduces the yield of maize hybrid seed (2). Therefore, the male-sterility line is critical for the commercial hybrid seed production in maize.

Male sterility mainly includes three types, i.e., cytoplasmic male sterility (CMS) caused by both mitochondrial and nuclear genes, genic male sterility (GMS) caused by nuclear genes alone, and photoperiod- and/or temperature-sensitive genic male sterility (2–4). Among them, the CMS-based three-line system has been successfully used for hybrid seed production in many crops (4). For example, the CMS hybrid rice has accounted for ∼40% of the total rice planting area in China since the late 1980s (5). However, the CMS system has suffered from several intrinsic problems, such as the limited genetic resources of the restorer lines, the low genetic diversity between the CMS lines and the restorer lines in rice (6), and the potentially increased disease susceptibility and unreliable restoration of CMS lines in maize (7). The photoperiod- and/or temperature-sensitive genic male sterility-based two-line system has been initially used for hybrid rice production in China since the 1990s (8). It eliminates the requirement for crossing to propagate the male-sterility female line, and almost any fertile line with a good combining ability can be used as a male parent, thus it can enhance the usage efficiency of genetic resources and further increase the yield of hybrid rice (3, 8). However, purity of hybrid seeds produced by using this system may be influenced by the undesired climate or environmental conditions (4).

The male gamete development is a well-orchestrated process; any disturbance may thus lead to male sterility (9). Up to now, more than 100 GMS genes have been identified in plants (2, 10, 11), and a great deal of effort has been made to develop biotechnology-based male-sterility systems by using these GMS genes and their

Significance

Developing a male-sterility system that is effective in multiple species is essential for hybrid seed production in different plants, especially for plants without cloned male-sterility genes. Here, we identified the transcriptional regulation mechanism for maize male-sterility gene *ZmMs7* and thereby developed a dominant male-sterility system that was proved to be effective in maize, rice, and *Arabidopsis*. Compared with current male-sterility systems, this system has potential advantages, e.g., utilization of a single transgene cassette, high stability of male sterility under different genetic backgrounds, and producing fluorescent transgenic and normal color nontransgenic F_1 hybrid seeds which can be used flexibly in different countries where transgenic crop cultivation is prohibited or allowed. Therefore, it is a simple, cost-effective, and multiple-crop-applicable biotechnology.

Author contributions: X.A., B.M., M.D., D. Yuan, L.Y., and X.W. designed research; X.A., B.M., Z.D., R.L., Q.H., S.W., D.Z., D.L., D. Yu, Y.Z., K.X., T.Z., S.Z., Y.T., C.L., and J.L. performed research; X.A., B.M., M.D., Z.D., Z.L., and X.W. analyzed data; and X.A., B.M., M.D., Z.D., and X.W. wrote the paper.

Reviewers: Q.Q., China National Rice Research Institute; and F.T., China Agricultural University.

The authors declare no competing interest.

[1]X.A., B.M., M.D., and Z.D. contributed equally to this work.

[2]To whom correspondence may be addressed. Email: lpyuan@hhrrc.ac.cn or wanxiangyuan@ustb.edu.cn.

This article contains supporting information online at https://www.pnas.org/lookup/suppl/doi:10.1073/pnas.2010255117/-/DCSupplemental.

First published September 9, 2020.

corresponding mutants to maintain and propagate GMS lines as female parents for hybrid seed production (2, 4). For instance, a system called seed production technology (SPT) was developed to produce recessive GMS lines by DuPont Pioneer using the maize *male sterility 45* (*ZmMs45*) gene, coupled with an *α-amylase* gene and a red fluorescence gene *DsRed* (12). Recently, we have updated the SPT system and developed the multi-control sterility (MCS) systems by using maize GMS genes *ZmMs7*, *ZmMs30*, and *ZmMs33*, respectively (13–15). A similar system was also constructed in rice (16). In addition, a dominant male-sterility system was developed to produce dominant GMS lines using the dominant GMS gene *ms44* in maize (17). Although these biotechnology-based male-sterility systems have several advantages (18), they rely on the combination of the cloned GMS genes and their corresponding mutants. Therefore, developing a male-sterility system would be a valuable application for hybrid seed production in various plant species, especially for plants without cloned GMS genes.

ZmMs7 encodes a PHD-finger transcription factor (TF) and is a key regulator of postmeiotic anther development in maize (13). Its orthologs have been identified in several plant species, such as *Arabidopsis male sterility 1* (*AtMS1*) (19–22), rice *male sterility 1*/*Persistent Tapetal Cell 1* (*OsMs1*/*OsPTC1*) (23, 24), and barley *male sterility 1* (*HvMs1*) (25). Mutations in *AtMs1* and *OsMs1*/*OsPTC1* result in abnormal tapetum programmed cell death (PCD) and defective pollen exine formation (22–24, 26). Both AtMs1 and OsMs1/OsPTC1 function as transcriptional activators (20, 23), and OsMs1/OsPTC1 interacts with tapetal regulatory factors, such as OsMADS15 and TDR Interacting Protein2 (TIP2), to regulate tapetal cell PCD and pollen exine formation (23). Both *HvMs1* and *OsPTC1* can functionally complement the *Arabidopsis ms1* mutation and rescue male fertility, indicating functions of AtMs1 orthologs in higher plants may be conserved (24, 25). Nevertheless, the precise molecular mechanism of transcriptional regulation by AtMs1 orthologs remains largely unknown.

Here, we investigate molecular mechanism of *ZmMs7* for regulating anther and pollen development, and find that ZmMs7 interacts with maize NF-Y subunits to form multiprotein complexes that directly activate target genes. Premature expression of *ZmMs7* driven by *p5126* results in the dominant and complete male sterility through dramatically altering the gene expression networks responsible for anther and pollen development. By using the *p5126-ZmMs7* transgenic element, we construct a dominant male-sterility (DMS) system that is proved to be effective in maize, rice, and *Arabidopsis*.

Results

***ZmMs7* Is Required for Tapetum Development and Pollen Exine Formation.** *ZmMs7* was cloned and verified by using functional complementation in our laboratory (13). To further confirm its function in controlling male fertility, four *ZmMs7* knockout lines were generated via the CRISPR-Cas9 system. Compared with wild type (WT), all of the *Cas9-ZmMs7* knockout lines displayed complete male sterility with no exerted anthers, and the shriveled anthers lacked pollen grains at mature stage, which is similar to the *ms7-6007* mutant (Fig. 1*A* and *SI Appendix*, Fig. S1), indicating that *ZmMs7* is required for male fertility in maize.

Maize anther development can be divided into 14 stages (stage 1 to stage 14) (2). To characterize the cytological defects in *ms7-6007* anthers, we performed scanning electron microscopy (SEM), transverse section, and transmission electron microscopy (TEM) analyses and found that anther and microspore development progressed similarly between WT and *ms7-6007* until stage 9 (Fig. 1 *B–D* and *SI Appendix*, Figs. S2–S4). The SEM analysis showed only transverse strips covered the outer surface of WT anthers until stage 10, and then the three-dimensional (3D) knitting cuticle formed at stage 11 and fully grew at stage 13. However, the 3D knitting cuticle appeared at stage 10 but gradually reduced thereafter in *ms7-6007* anthers. On the inner surface, Ubisch bodies emerged at stage 9 in both WT and *ms7-6007* anthers, and they enlarged subsequently in WT but gradually disappeared in *ms7-6007* (*SI Appendix*, Fig. S2). The transverse section analysis showed developmental differences between WT and *ms7-6007* anthers occurred after stage 9. For example, at stage 11, the vacuoles disappeared in the microspore and tapetal cells almost completely degenerated in WT anthers, while the mutant locules started to shrink and the microspores broke (Fig. 1*B* and *SI Appendix*, Fig. S3). Similarly, the SEM observation of pollen showed that microspore mother cells, dyads, tetrads, and microspores were successively generated from stages 7 to 9 in both WT and *ms7-6007* anthers. After formation of the vacuolated microspores at stage 10, starch granules were gradually accumulated, and then the regular round-shaped mature pollen grains formed in WT anther locules at stage 13. By contrast, the *ms7-6007* vacuolated microspores severely sank at stage 10 and disappeared at stage 12 (Fig. 1*C* and *SI Appendix*, Fig. S3). The TEM observation showed that Ubisch bodies appeared on the inner surface of WT and mutant anthers at stage 9, enlarged thereafter in WT, but not enlarged in *ms7-6007*. The WT microspores were enveloped with evident exine at stage 9, and then their distinctive layers (i.e., tectum, bacula, and foot layer) formed and thickened from stages 10 to 13. However, the *ms7-6007* exine was much thinner than that of WT (Fig. 1 *D* and *E* and *SI Appendix*, Fig. S4). Taken together, loss of function of *ZmMs7* results in delayed tapetal degeneration, abnormal Ubisch body development, and pollen wall formation, and these developmental defects ultimately cause complete male sterility.

ZmMs7 Functions as a Transcriptional Activator and Regulates Genes Involved in Tapetum Development and Pollen Exine Formation. The spatiotemporal expression patterns of *ZmMs7* in different tissues were detected by using real-time quantitative PCR (RT-qPCR). *ZmMs7* transcript was only detected in WT anthers from stages 8b to 10, and peaked at stage 9, indicating that *ZmMs7* is specifically expressed in maize anthers at tetrad and free haploid microspore stages (Fig. 2*A*). *ZmMs7* encodes a PHD-finger protein (13) which is localized in the nucleus, supporting that it functions as a TF (Fig. 2*B*). ZmMs7 dramatically enhanced the reporter expression in a transient dual-luciferase reporter assay performed in maize protoplasts, indicating that ZmMs7 has a transcriptional activation activity (Fig. 2*C*). To further test the transcriptional activity in planta, *ZmMs7* was fused with a conserved suppressing motif, SRDX (LDLDLELRLGFA), which can convert transcriptional activators into dominant repressors (27). Transformation of *pZmMs7:ZmMS7-SRDX* into maize plants inhibited anther and pollen development, and led to complete male sterility (Fig. 2*D*). These results strongly suggest that ZmMs7 acts as a transcriptional activator in maize anthers, being consistent with its homologs AtMs1 (20) and OsMs1/OsPTC1 (23), implying that ZmMs7-mediated transcriptional regulatory mechanism may be conserved among different plant species.

To identify the downstream genes potentially regulated by *ZmMs7* during anther development, RNA sequencing (RNA-seq) analysis was performed using WT and *ms7-6007* anthers at stages 8 to 10 (*SI Appendix*, Fig. S5*A*). A total of 1,143 differentially expressed genes (DEGs) between WT and *ms7-6007* were detected (*SI Appendix*, Fig. S5 *B–F*). Among these DEGs, 710 were down-regulated and 809 were up-regulated in *ms7-6007* anthers during at least one stage (Fig. 2*E* and *SI Appendix*, Table S1). Gene ontology analysis of the 1,143 DEGs showed that *ZmMs7* modulates biological processes such as pollen exine formation, polysaccharide catabolism, phenypropanoid biosynthesis, and cell differentiation processes, most of which are important for anther and pollen development (*SI Appendix*, Fig. S5*G*). Particularly, a set of genes putatively related to tapetum and pollen wall development showed altered expression patterns in *ms7-6007* anthers, including *ZmMs45* (28), *Indeterminate Gametophyte1* (*IG1*) (29), *IG1*/*AS2-like1* (*IAL1*) (29), *maize basic Helix–loop–helix 122* (*ZmbHLH122*) (30), *maize*

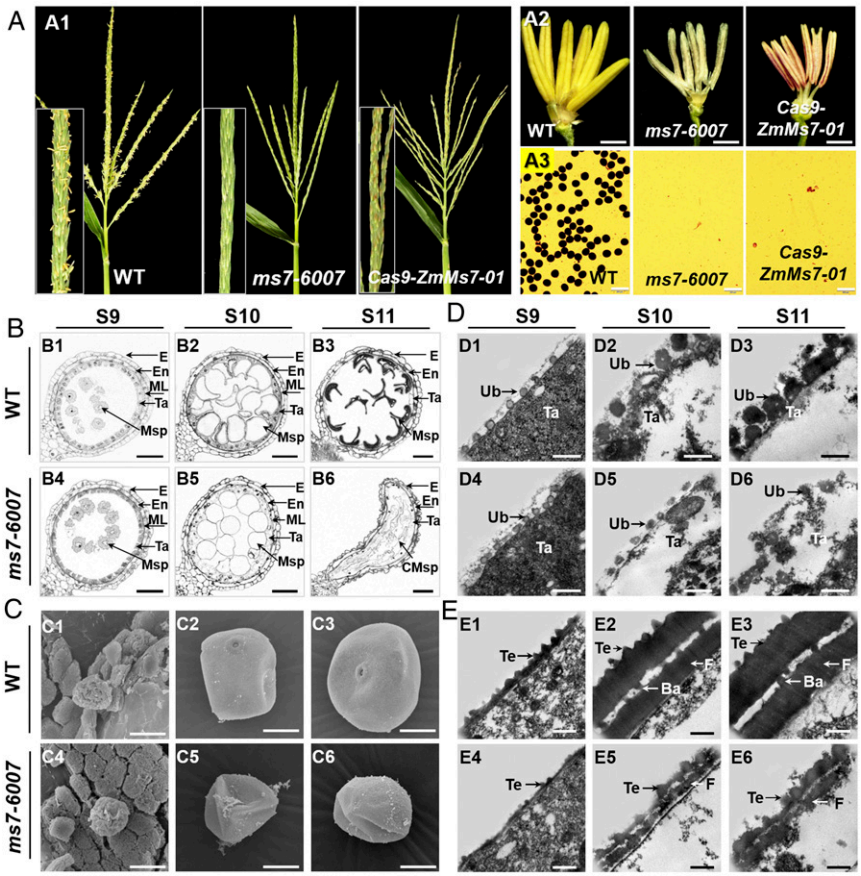

Fig. 1. Phenotypic and cytological comparison of WT, *ms7-6007* mutant, and *ZmMs7* knockout line generated via the CRISPR-Cas9 method. (*A*) Comparison of tassels (A1), anthers (A2), and pollen grains stained with I_2-KI (A3) among WT, *ms7-6007* mutant, and the *Cas9-ZmMs7-01* line. (Scale bars, 1 mm in A2 and 200 μm in A3.) (*B*) Transverse section analysis of anthers in WT (B1 to B3) and *ms7-6007* mutant (B4 to B6) from stages 9 to 11 during maize anther development. (Scale bar, 50 μm.) (*C*) SEM analysis of pollen grain development in WT (C1 to C3) and *ms7-6007* mutant (C4 to C6). (Scale bar, 20 μm.) (*D*) TEM analysis of Ubisch body in WT (D1 to D3) and *ms7-6007* mutant (D4 to D6). (Scale bar, 0.5 μm.) (*E*) TEM analysis of pollen exine in WT (E1 to E3) and *ms7-6007* mutant (E4 to E6) (Scale bar, 0.5 μm.) Ba, bacula; CMsp, collapsed microspore; E, epidermis; En, endothecium; F, foot layer; ML, middle layer; Msp, microspore; Ta, tapetum; Te, tectum; and Ub, Ubisch body.

Metallothionein 2C (*ZmMT2C*) (31), *maize Aspartyl Protease 37* (*ZmAP37*) (32), *ZmMs6021*, *maize Dihydroflavonol 4-Reductase-Like 1/2* (*ZmDRL1/2*), *maize Less Adhesive Pollen 5* (*ZmLAP5*), *maize Acyl-COA-Synthetase 5* (*ZmACOS5*), and *maize Quartet3* (*ZmQRT3*) (2, 11) (*SI Appendix*, Tables S1–S4).

Since a set of lipid metabolism-related genes displayed altered expression patterns in *ms7-6007* anthers (*SI Appendix*, Table S1), the components of cutin, wax, and internal fatty acids in WT and *ms7-6007* anthers were detected. The results showed a dramatic reduction for the total cutin content and most of the cutin monomers in *ms7-6007* anthers (Fig. 2*F* and *SI Appendix*, Fig. S6*A* and Table S2). No significant difference was detected for the total wax and internal fatty acid contents between WT and *ms7-6007* anthers (Fig. 2 *F* and *G*), although most of the individual components of wax and internal fatty acids displayed significant changes (*SI Appendix*, Fig. S6 *B* and *C*). These results suggested that *ms7-6007* mutation impedes cutin biosynthesis and alters the constituents of wax and internal fatty acids, thereby affecting anther wall development and pollen exine formation.

ZmMs7 Forms Multiprotein Complexes with ZmNF-Y Subunits. Like many PHD finger proteins, ZmMs7 has no DNA binding domain as analyzed by the InterPro online program (https://www.ebi.ac.uk/interpro/). To understand how ZmMs7 regulates its target genes, we used yeast two-hybrid (Y2H) assay to screen its interactors. Because the C-terminal domain of ZmMs7 possesses self-activation activity, the N-terminal region (amino acids 1 to 358) was used as bait for the Y2H assay. A total of 130 positive clones were obtained, and four NF-Y proteins were confirmed to interact with ZmMs7, including ZmNF-YA6, ZmNF-YC9, ZmNF-YC12, and ZmNF-YC15 (Fig. 3 *A*, *Left* and *SI Appendix*, Fig. S7 *A* and *C*). To validate these protein interactions, coimmunoprecipitation (Co-IP) assay was performed in maize protoplasts. The four NF-Y proteins were strongly coimmunoprecipitated by ZmMs7-cYFP-Myc, suggesting that ZmMs7 physically links the NF-YA6 and NF-YC9/12/15 subunits in plant cells (Fig. 3 *A*, *Right*). Bimolecular fluorescence complementation (BiFC) assay in maize protoplasts further conformed the results (Fig. 3*D*). Since NF-Y TFs are reported to form heterotrimeric complexes composed of NF-YA, NF-YB, and NF-YC subunits (33), the interactions between NF-YA and NF-YC subunits were tested by using Y2H, Co-IP, and BiFC assays. The results showed that NF-YA6 can interact with all of the three NF-YC9/12/15 subunits in both yeast and plant cells (Fig. 3 *B* and *D*). Next, to find out the NF-YB counterparts of the NF-Y complexes, we conducted Y2H screening between candidate NF-YBs and ZmMs7, NF-YA6 and NF-YC9/12/15. Among 18 NF-YB members of maize (34), NF-YB2 was found to interact with NF-YC9/12/15, but not with NF-YA6 and ZmMs7, which was further confirmed by Co-IP and BiFC assays (Fig. 3 *C* and *D*). Besides NF-YB2, NF-YB10 was found to interact with NF-YC15, but not with NF-YC9/12 (*SI Appendix*, Fig. S8). Therefore, we selected NF-YB2 for further

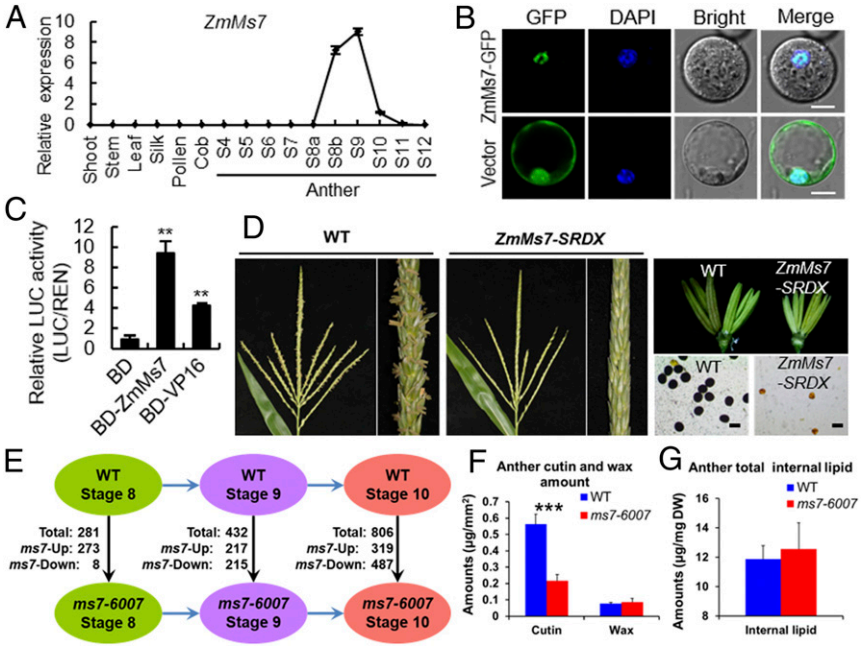

Fig. 2. Gene expression, transcriptional activity, and transcriptome and lipidome analyses of *ZmMs7*. (*A*) RT-qPCR analysis of *ZmMs7* expression in different organs of maize. Data are means ± SD, $n = 3$. (*B*) Subcellular localization of ZmMs7 in maize protoplasts. DAPI staining was used as a nuclear marker. (Scale bar, 10 μm.) (*C*) Transcriptional activation assay of ZmMs7 using a dual-luciferase system in maize protoplasts. GAL4 DNA binding domain (BD) and transcriptional activator VP16 were used as negative and positive controls, respectively. Data are means ± SD, $n = 4$. Asterisks indicate significant difference compared to BD (**$P < 0.01$, Student's *t* test). (*D*) Male sterile phenotype of *pZmMs7:ZmMS7-SRDX* transgenic maize plants. Comparison of tassels, anthers, and pollen grains stained with I_2-KI between WT and transgenic plants. (Scale bar, 100 μm.) (*E*) The numbers of DEGs between WT and *ms7-6007* mutant anthers at stages 8, 9, and 10, respectively. (*F*) Total amount of anther cutin and wax per unit surface area and (*G*) total amount of anther internal lipid per dry weight (DW) in WT and *ms7-6007* mutant. Data are means ± SD, $n = 5$. Asterisks indicate significant difference in comparison (***$P < 0.001$, Student's *t* test).

studies. Meanwhile, the RT-qPCR analysis showed that *NF-YA6*, *NF-YB2*, and *NF-YC9/12/15* genes were all expressed in maize anthers during stages 6 to 10 (*SI Appendix*, Fig. S7*D*). The coexpression patterns of *ZmMs7* and *NF-Y* genes provided a prerequisite for the protein interactions between ZmMs7 with NF-Y subunits in maize anthers. Together, ZmMs7 can form protein complexes with NF-YA6, NF-YB2, and NF-YC9/12/15 (Fig. 4*F*).

The ZmMs7-NF-Y Complexes Directly Activate Target Gene Expression. To identify target genes of ZmMs7, we selected a set of genes with down-regulated expressions in *ms7-6007* anther, including *ZmMs6021*, *ZmIAL1*, *ZmMT2C*, *ZmAP37*, and *ZmQRT3* that are homologous to the reported GMS genes in rice and *Arabidopsis*. Among these genes, the *ZmMT2C* promoter was significantly activated by the ZmMs7-NF-Y complexes in the transactivation assay, suggesting that ZmMs7 in cooperation with ZmNF-YA6-YB2-YC9/12/15 trimers activates the *ZmMT2C* promoter in maize protoplasts (Fig. 4*A*). Considering that *ZmMT2C* is potentially involved in tapetum development, we selected this gene for further testing. It was reported that NF-Y complex binds to the consensus motif CCAAT in the promoters of target genes (33). Electrophoretic mobility shift assays (EMSA) showed that MBP-NF-YA6 can specifically bind to the CCAAT box in the promoter region of *ZmMT2C* (Fig. 4*B*). Next, to examine whether ZmMs7 complexes can bind to the *ZmMT2C* promoter in vivo, we performed chromatin immunoprecipitation quantitative PCR (ChIP-qPCR) analysis using the anther samples of *ZmMs7-3xMyc* transgenic maize plants. Compared with the control probes (P2 and P3), the P1 fragment containing the CCAAT box was significantly enriched by using anti-*c*-Myc antibody (Fig. 4*C*), suggesting that ZmMs7 binds to the *ZmMT2C* promoter in vivo through association with the CCAAT element. Collectively, ZmMs7-NF-Y complexes can directly activate expression of the target gene *ZmMT2C*.

Since *ZmMT2C* is a homolog of *OsMT2b* which is involved in tapetal cell PCD of rice anthers (31), we examined DNA fragmentation in WT and *ms7-6007* anthers using a terminal deoxynucleotidyl transferase-mediated dUTP nick-end labeling (TUNEL) assay. TUNEL signals began to appear at stage 9 in WT anthers, but later appeared at stage 10 in *ms7-6007* anthers, indicating that tapetal cell PCD is delayed in *ms7-6007* anthers (Fig. 4*D*). Consistent with the TUNEL results, the TEM analysis showed delayed tapetum degeneration in *ms7-6007* anthers compared with that in WT (Fig. 4*E*). Collectively, *ZmMs7* may regulate tapetal cell PCD via directly activating the expression of its target gene *ZmMT2C* and modulate anther cuticle and pollen wall formation by indirectly regulating cutin and sporopollenin biosynthesis-related genes such as *ZmMs6021*, *ZmDRL1/2*, *ZmLAP5*, and *ZmACOS5* (Fig. 4*F*).

***ms7-6007* Mutation Is Genetically Stable and Applicable for Hybrid Maize Breeding and Seed Production.** A total of 403 maize inbred lines with broad genetic diversity were used to test whether male sterility caused by *ms7-6007* mutation was stable under different maize germplasms (*SI Appendix*, Fig. S9*A* and Table S3). The 403 lines were pollinated by pollen of heterozygous plants (*ZmMs7/ms7-6007*) and then 403 F_2 populations were generated from the self-pollination of F_1 plants with the genotype of *ZmMs7/ms7-6007* based on marker-assisted selection. Among the 403 F_2 populations, 376 (93.3%) type II populations ($0.05 < P$ values ≤ 1.0 and $1.6 <$ ratios ≤ 7.0) fitted to the 3:1 ratio of fertile plants to sterile plants, while six (1.5%) type I ($0 \leq P$ values < 0.05 and $1.2 <$ ratios ≤ 1.6) and 21 (5.2%) type III populations ($0 \leq P$ values < 0.05 and $7.0 <$ ratios ≤ 42.0) showed segregation deviated from the expected 3:1 ratio (*SI Appendix*, Fig. S9*B* and Table S3). To justify whether the deviated segregation from 3:1 in the 27 type

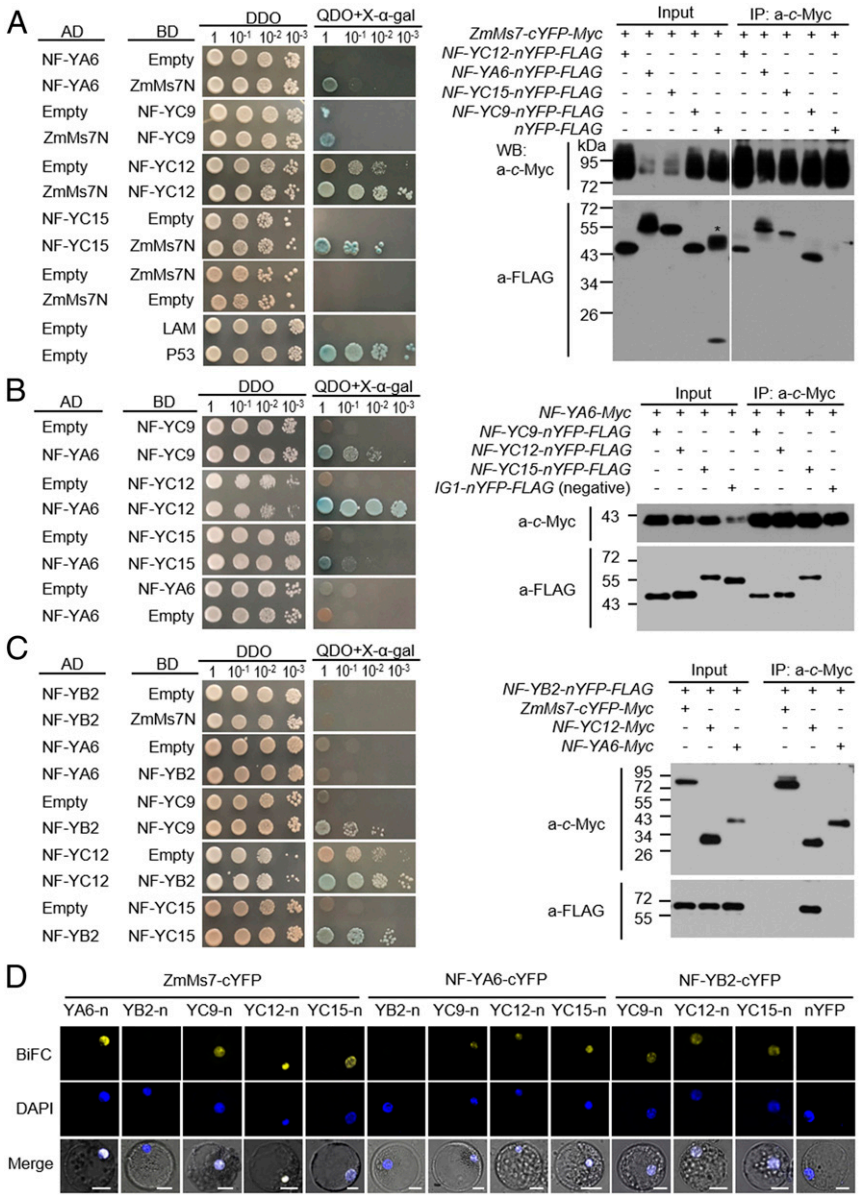

Fig. 3. Interaction of ZmMs7 with ZmNF-Y subunits. (*A*) Y2H and Co-IP assays of ZmMs7 interaction with NF-YA6 and NF-YC9/12/15. For Y2H assay, LAM and P53 were used as negative and positive controls, respectively. DDO, double dropout medium (SD-Trp-Leu); QDO, quadruple dropout medium (SD-Trp-Leu-His-Ade). Co-IP assays were performed using a transient expression system in maize protoplasts; the *nYFP-FLAG* was used as a negative control. The asterisk indicates a nonspecific band. (*B*) Y2H and Co-IP assays of NF-YA6 interaction with NF-YC9/12/15. *IG1-nYFP-FLAG* was used as a negative control. Others are as in *A*. (*C*) Y2H and Co-IP assays of NF-YB2 interaction with ZmMs7N, NF-YA6, and NF-YC9/12/15. Others are as in *A*. (*D*) BiFC analysis of in vivo interaction between ZmMs7, NF-YA6, NF-YB2, and NY-YC9/12/15 in maize protoplasts. Protein name-n indicates nYFP fusions. DAPI staining was used as a nuclear marker. The fluorescence was detected using confocal microscopy. (Scale bar, 10 μm.)

I and III populations may result from environmental conditions or the exogenetic fertile pollen unexpectedly participating in the self-pollination of the 27 F_1 plants, we randomly chose 4 from the 27 type I and III populations and performed molecular marker analysis using a *ms7-6007* mutation marker. Interestingly, we found that the male-sterility genotypes of 4 F_2 populations matched well with their corresponding sterile phenotypes (*SI Appendix*, Fig. S9*C*), indicating that male sterility of the *ms7-6007* mutation is stable in the 27 populations with deviated segregation from 3:1. Additionally, the tassels of sterile F_2 individuals were collected from 8 F_2 populations with different tassel shapes from those of WT and *ms7-6007* and showed complete male sterility and no anther shedding. Moreover, no pollen grain was observed in the anthers of these sterile individuals under different genetic backgrounds, which resembled the *ms7-6007* mutant (*SI Appendix*, Fig. S9*D*). Therefore, male sterility of the *ms7-6007* mutation is stable under diverse maize genetic backgrounds.

To test whether *ms7-6007* mutation affects grain yield and other agronomic traits in hybrid maize production, we randomly selected 31 elite inbred lines and took them as male parents to cross with the *ZmMs7*/*ZmMs7* and *ms7-6007*/*ms7-6007* homozygous plants, respectively. The harvested F_1 hybrids and their corresponding parental lines were grown in three locations in triplicate. Seventeen agronomic traits were investigated to compare the differences of heterosis and field production performance between each of the 31 pairs of hybrid combinations (*SI Appendix*, Table S4). The hybrids derived from *ms7-6007* and its WT as female parents showed similar field performance in the

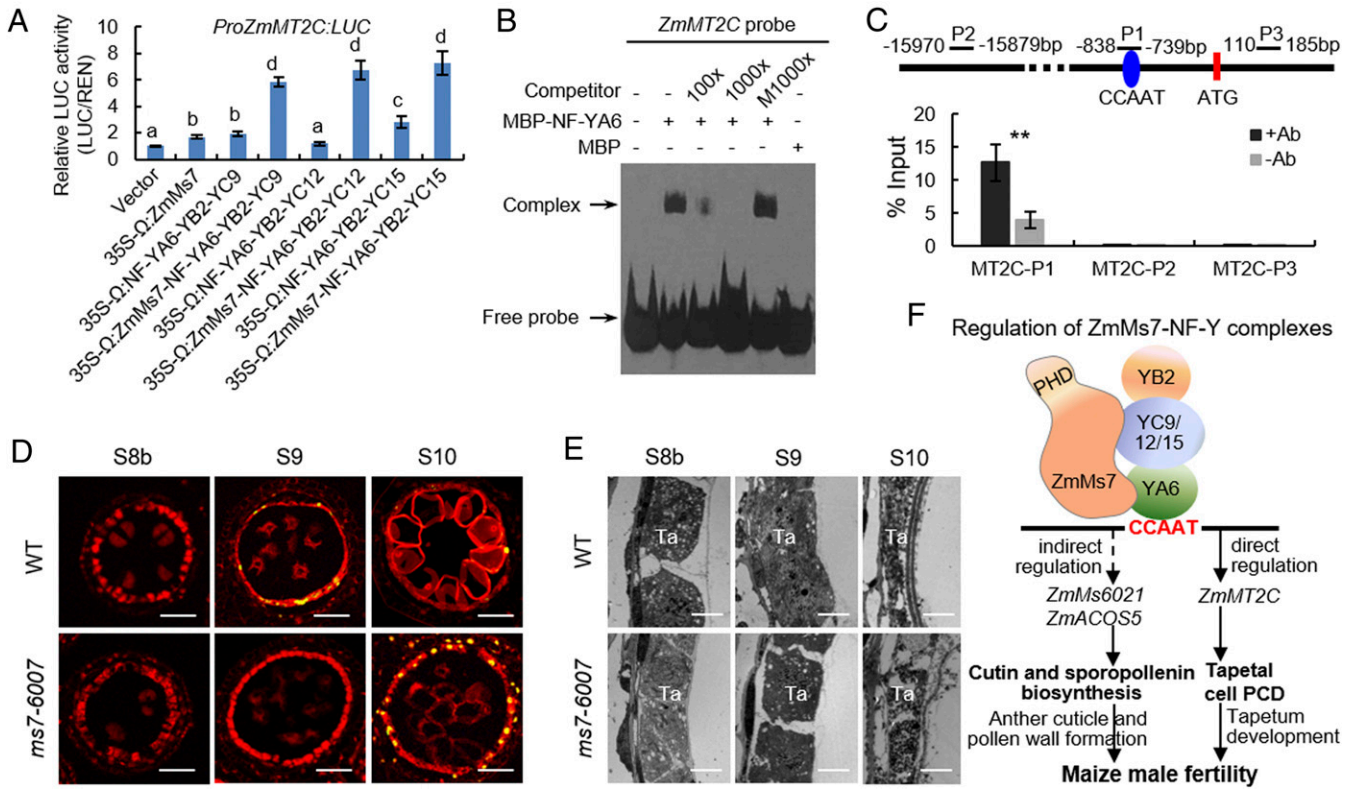

Fig. 4. ZmMs7-NF-YA/YB/YC complexes directly activate target gene expression. (*A*) Transient dual-luciferase assay of *ZmMT2C* promoter activity activated by ZmMs7-NF-Y complexes in maize protoplasts. Data are means ± SD, $n = 3$. Different letters above each column indicate significant difference ($P < 0.01$, Student's *t* test). (*B*) EMSA assay of ZmNF-YA6 binding to the CCAAT box in *ZmMT2C* promoter region. (*C*) The enrichments of *ZmMT2C* promoter analyzed by ChIP-qPCR with the primer sets (P1, P2, and P3), using the anther samples of *ZmMs7-3x Myc* transgenic maize plants. Data are means ± SD, $n = 3$. +Ab, presence of anti-c-Myc antibody; −Ab, absence of the antibody. The asterisks indicate significant difference between +Ab and −Ab ($P < 0.01$, Student's *t* test). (*D*) Detection of DNA fragmentation by TUNEL assay in WT and *ms7-6007* anthers. (Scale bar, 50 μm.) (*E*) TEM of tapetum degeneration in WT and *ms7-6007* anthers. Ta, tapetum. (Scale bar, 10 μm.) (*F*) Model of ZmMs7-NF-YA/YB/YC complexes controlling maize male fertility through directly activating *ZmMT2C* expression and indirectly regulating cutin and sporopollenin biosynthesis-related genes such as *ZmMs6021*, *ZmLAP5*, *ZmDRL1/2*, and *ZmACOS5*.

three locations (*SI Appendix*, Fig. S10). The plot yields of 13 representative pairs of hybrid combinations, and ear morphologies of 4 pairs of hybrid combinations were shown in *SI Appendix*, Figs. S11 and S12*A*, as examples. All of the hybrid combinations greatly outperformed their parents, whereas plot yields showed almost no statistical difference between pairs of the 31 hybrid combinations (*SI Appendix*, Table S4). For other important traits, such as 100-seed weight, grain number per ear, plant height, and mature period, significant differences between a few pairs of hybrid combinations were detected under only one environmental condition. Nevertheless, the change trends showed complete randomness between pairs of the 31 hybrid combinations (*SI Appendix*, Fig. S12 *B–E* and Table S4). These results demonstrated that the *ms7-6007* mutation has no obvious negative effects on maize heterosis and field production, suggesting that the *ZmMs7* gene and its mutant *ms7-6007* are applicable for hybrid maize breeding and seed production.

Premature Expression of *ZmMs7* Driven by an Anther-Specific Promoter *p5126* Disrupts Tapetum and Pollen Development and Results in Dominant Male Sterility in Maize. The maize anther-specific promoter *p5126* confers tapetal-specific expression at stages 7 to S8a (28) which is earlier than the expression of *ZmMs7* at stages 8b to 10. Overexpression of *ZmMs7* homologous genes, *AtMs1* and *HvMS1*, results in dominant male sterility in *Arabidopsis* and barley, respectively, indicating precise control of *AtMs1* and *HvMS1* expression is critical for male fertility in plants (22, 25). Therefore, to develop a dominant male-sterility system, we constructed the *p5126-ZmMs7M* vector containing three functional modules, i.e., *ZmMs7* expression cassette driven by *p5126* to obtain a dominant male-sterility trait, the red fluorescence protein gene *mCherry* driven by the aleurone-specific *LTP2* promoter to mark the color of transgenic seeds, and the herbicide-resistant gene *Bar* driven by the *CaMV35S* promoter to select transgenic plants (*SI Appendix*, Fig. S13*A*). As a result, five *p5126-ZmMs7M* transgenic events (*p5126-ZmMs7M-01* to *-05*) showed dominant male sterility with smaller anthers and no pollen grain, whereas their vegetative development and female fertility were normal (Fig. 5*A* and *SI Appendix*, Fig. S13*B*). Due to the dominant male sterility, the *p5126-ZmMs7M* element can be genetically transmitted only through female gametes. Thus all of the transgenic lines produced nearly 50% transgenic fluorescent seeds and 50% nontransgenic normal color seeds as observed under green excitation light with different red fluorescence filters (Fig. 5*B* and *SI Appendix*, Fig. S13*B*).

Microscopic analyses were conducted to explore the morphological defects of anther and pollen in the *p5126-ZmMs7M-01* line. The SEM analysis showed that the 3D knitting cuticle formed at stage 11 in both WT and *p5126-ZmMs7M-01* anthers. But it was obviously tighter and thinner in *p5126-ZmMs7M-01* anthers. On the inner surface of the *p5126-ZmMs7M-01* anther wall, lots of lipid droplets emerged evidently at stage 9, but no typical Ubisch body was observed when compared with that of WT (*SI Appendix*, Fig. S2). The transverse section analysis showed that obvious differences between WT and *p5126-ZmMs7M-01* anthers started to appear at stage 9. At this stage, abnormal tapetal cell proliferation and swelling occurred evidently in *p5126-ZmMs7M-01*

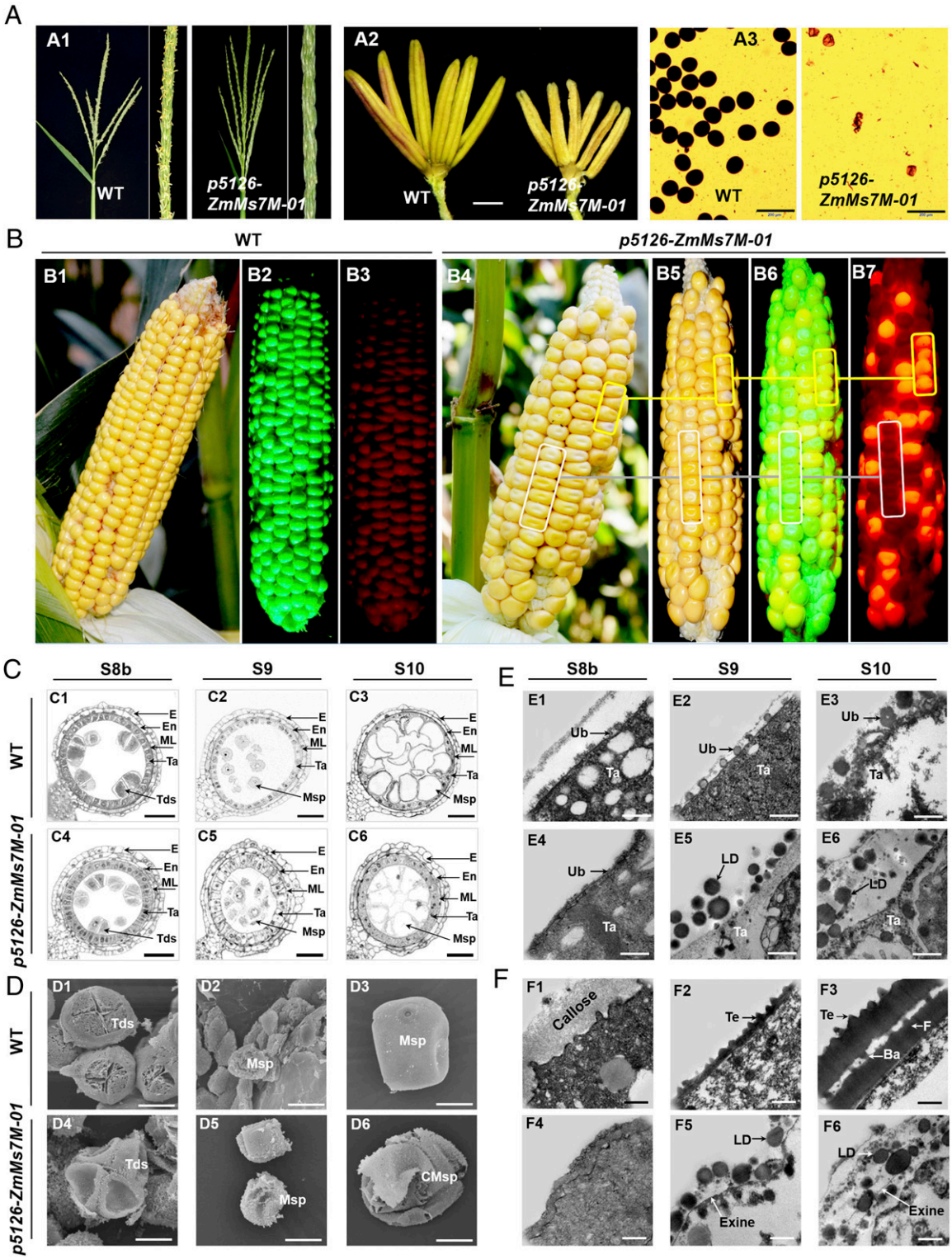

Fig. 5. Phenotypic and cytological comparison of WT and the *p5126-ZmMs7M-01* dominant male-sterility line. (*A*) Comparison of tassels (A1), anthers (A2), and pollen grains stained with I_2-KI (A3) between WT and the *p5126-ZmMs7M-01* line. (Scale bars, 1 mm in A2 and 200 μm in A3.) (*B*) Comparison of ear phenotypes between WT and the *p5126-ZmMs7M-01* line under bright light (B1, B4, and B5) and green excitation light with red fluorescence filter I (GREEN.L, China) (B2 and B6) and red fluorescence filter II (NIGHTSEA, United States) (B3 and B7). (*C*) Transverse section analysis of anthers in WT (C1 to C3) and the *p5126-ZmMs7M-01* line (C4 to C6) from stage 8b to 10 during maize anther development. (Scale bar, 50 μm.) (*D*) SEM analysis of microspores in WT (D1 to D3) and the *p5126-ZmMs7M-01* line (D4 to D6). (Scale bar, 20 μm.) (*E*) TEM analysis of Ubisch body in WT (E1 to E3) and the *p5126-ZmMs7M-01* line (E4 to E6). (Scale bar, 0.5 μm.) (*F*) TEM analysis of pollen exine in WT (F1 to F3) and the *p5126-ZmMs7M01* line (F4 to F6). (Scale bar, 0.5 μm.) Ba, bacula; CMsp, collapsed microspore; E, epidermis; En, endothecium; F, foot layer; LD, lipid droplet; ML, middle layer; Msp, microspore; Ta, tapetum; Tds, tetrads; Te, tectum; and Ub, Ubisch body.

anthers. At stage 10, WT tapetum showed the hill-like structures indicating the degeneration of tapetal cells, while *p5126-ZmMs7M-01* tapetum maintained a regular shape without degeneration. Another locule of *p5126-ZmMs7M-01* line started to shrink at stage 11, and ultimately formed a similar shape with that of *ms7-6007* at stage 13 (Fig. 5*C* and *SI Appendix*, Fig. S3). Meanwhile, the SEM analysis of pollen showed that microspore mother cells, dyads, tetrads, and microspores were successively generated in *p5126-ZmMs7M-01* anthers. However, the haploid microspores sank severely in the tetrads at stage 8b, the integrity of the microspore cell wall was disrupted at stage 10, and only cell debris remained within the locule of *p5126-ZmMs7M-01* anthers from stages 11 to 13 (Fig. 5*D* and *SI Appendix*, Fig. S3). The TEM analysis showed that the obvious Ubisch bodies appeared at stage 9 and gradually enlarged from stages 10 to 13 on the inner surface of WT tapetum. However, lots of lipid droplets instead of Ubisch bodies accumulated on the inner surface of *p5126-ZmMs7M-01* tapetum from stages 9 to 11 (Fig. 5*E* and *SI Appendix*, Fig. S4). Similarly, lipid droplets were observed on the *p5126-ZmMs7M-01* microspore wall from stages 9 to 13, and no obvious exine was found when compared with that in WT (Fig. 5*F* and *SI Appendix*, Fig. S4). Taken together, premature expression of *ZmMs7* driven by *p5126* disrupts tapetum and pollen wall development, which accounts for the dominant male sterility of the *p5126-ZmMs7M-01* line.

Premature Expression of *ZmMs7* Alters Expression Patterns of Genes Required for Tapetum and Pollen Development in Maize. To investigate the molecular basis underlying the dominant male sterility, anther transcriptomes of WT and the *p5126-ZmMs7M-01* line were analyzed and compared during six developmental stages (S6 to S10) based on RNA-seq. At the six investigated stages, 62.3% (5,390/8,654) of DEGs were found to be up-regulated in *p5126-ZmMs7M-01* anthers, being consistent with the activator function of ZmMs7. Among the 4,474 individual DEGs identified in *p5126-ZmMs7M-01* anthers from stages 6 to 10, 492 genes were overlapped with the 1,143 DEGs identified in *ms7-6007* anthers (*SI Appendix*, Fig. S14 *A–C*). The 492 shared DEGs were functionally enriched in pollen development and the exine formation process, which is consistent with the defective pollen wall phenotypes of the *p5126-ZmMs7M-01* line (Fig. 5 *C–F* and *SI Appendix*, Fig. S14*D*). Because ZmMs7 acts as a transcriptional activator, to examine the direct effects of *ZmMs7* premature expression on its downstream targeted or regulated genes, we identified 126 shared genes that were down-regulated in *ms7-6007* anthers at all three stages (stages 8 to 10), but up-regulated in *p5126-ZmMs7M-01* anthers from stages 7 to S8b (Fig. 6*A* and *SI Appendix*, Fig. S16 and Tables S5 and S6). The 126 genes were functionally enriched in biological processes such as cellular development, cell differentiation, lipid biosynthesis, and transmembrane transport, which are critical for development of the anther, tapetum, and pollen wall (Fig. 6*B*). To further confirm the transcriptomic results, we performed RT-qPCR analysis on six genes including *ZmMs7*, one target gene (*ZmMT2C*) regulated by ZmMs7-NF-Y complexes, and four GMS homologous genes (*ZmAP37*, *ZmQRT3*, *ZmIAL1*, and *ZmMs6021*) (Fig. 6*C*). *ZmMs7* expression peaked at stage 9 in WT anther and at stage 8a in *p5126-ZmMs7M-01* anther, showing that *ZmMs7* expression was advanced by two stages in the *p5126-ZmMs7M-01* line. Consistently, the expression peaks of *ZmMT2C*, *ZmAP37*, *ZmQRT3*, and *ZmMs6021* were advanced by one to two stages in the *p5126-ZmMs7M-01* line. The transcript level of *ZmIAL1* was obviously elevated from stages 8b to 10 in the *p5126-ZmMs7M-01* line (Fig. 6*C*). Collectively, the premature expression of *ZmMs7* driven by *p5126* altered expression patterns of genes involved in tapetum and pollen development, which likely led to the dominant male sterility of *p5126-ZmMs7M* lines.

Construction of a Dominant Male-Sterility System Based on the Conserved Function of *p5126-ZmMs7* in Maize, Rice, and *Arabidopsis*. Functions of *ZmMs7* and its orthologs have been found to be conserved in *Arabidopsis*, maize, rice, and barley (13, 19, 24, 25). This prompted us to further test whether premature expression of *ZmMs7* can induce similar dominant male sterility in other plant species. Firstly, the plasmid of *p5126-ZmMs7M* was transformed into rice. The obtained four T_0 transgenic rice lines exhibited normal vegetative growth and spikelet morphology, but their anthers were smaller and whitish, lacking viable pollen grains (Fig. 7*A*), indicating that the *p5126-ZmMs7M* element causes dominant male sterility in rice. The transgenic element can be transmitted through the female gamete when pollinated by WT pollen, and the harvested panicles contained about 50% of T_1 fluorescent seeds with a hemizygous transgenic genotype (*p5126-ZmMs7M/-*) and 50% T_1 normal color seeds without the transgene (Fig. 7*A*). Secondly, the plasmid *p5126-ZmMs7-myc* was introduced into *Arabidopsis*. The obtained three T_1 transgenic events developed as WT except that their siliques were stunted and failed to set seeds (Fig. 7*B*). Abundant pollen grains were observed on WT stigma after anther dehiscence. In contrast, the anthers of the three transgenic *Arabidopsis* plants became brown and had few pollen grains without germination ability (Fig. 7*B*). Taken together, the dominant male sterility induced by premature expression of *ZmMs7* is conserved in both monocot (e.g., maize and rice) and dicot (e.g., *Arabidopsis*). This type of biotechnology-based male sterility is thus proposed as a DMS system in plants. The detailed strategy is shown in *SI Appendix*, Fig. S13*C* using maize as an example.

Additionally, the stability of dominant male sterility caused by premature expression of *ZmMs7* was evaluated by crossing the *p5126-ZmMs7M-01* line with 392 maize inbred lines with broad genetic diversity (*SI Appendix*, Fig. S15*A* and Table S7). Then the fluorescent and normal color seeds in each of 392 F_1 populations were manually sorted out and grown separately. All plants exhibited normal vegetative growth and female fertility. Plants from normal color seeds in all of the 392 F_1 populations were male fertile, while plants from fluorescent seeds of 391 F_1 populations were male sterile without exerted anthers and pollen grain (*SI Appendix*, Fig. S15 *B–D*). One exception was that plants from fluorescent seeds of the C460 F_1 population showed male fertility, and the reason may be that the transgenic element *p5126-ZmMs7M* was disrupted or silenced in the C460 line. Nevertheless, the dominant male sterility induced by *p5126-ZmMs7M* is relatively stable under different maize genetic backgrounds.

Discussion

In this study, we investigated molecular regulation by ZmMs7 required for maize male fertility and hereby developed a DMS system. ZmMs7 acts as a transcriptional activator and interacts with ZmNF-Y subunits to form multiprotein complexes which are capable of activating downstream genes directly. Most interestingly, premature expression of *ZmMs7* driven by *p5126* altered the expression patterns of a series of genes involved in tapetum and pollen development and thus led to dominant male sterility in maize. As *ZmMs7* is a key regulator of anther and pollen development, and the regulatory pathways by *ZmMs7* orthologs are conserved among different plant species, we successfully developed an applicable DMS system by using the *p5126-ZmMs7* transgenic element in maize, rice, and *Arabidopsis*.

ZmMs7 orthologs have been identified in several plant species, including *AtMs1* (19–22), *OsMs1*/*OsPTC1* (23, 24, 31), and *HvMs1* (25). Nevertheless, the precise molecular mechanisms and direct target genes of these TFs remain largely unknown. Here, Y2H, Co-IP, and BiFC assays revealed that ZmMs7 can interact with ZmNF-Y subunits to form three ZmMs7-NF-YA6-YB2-YC9/12/15 complexes, suggesting that ZmMs7 achieves its transcriptional regulatory function through interaction with other TFs. The NF-Y heterotrimeric TFs are found in all eukaryotes. In

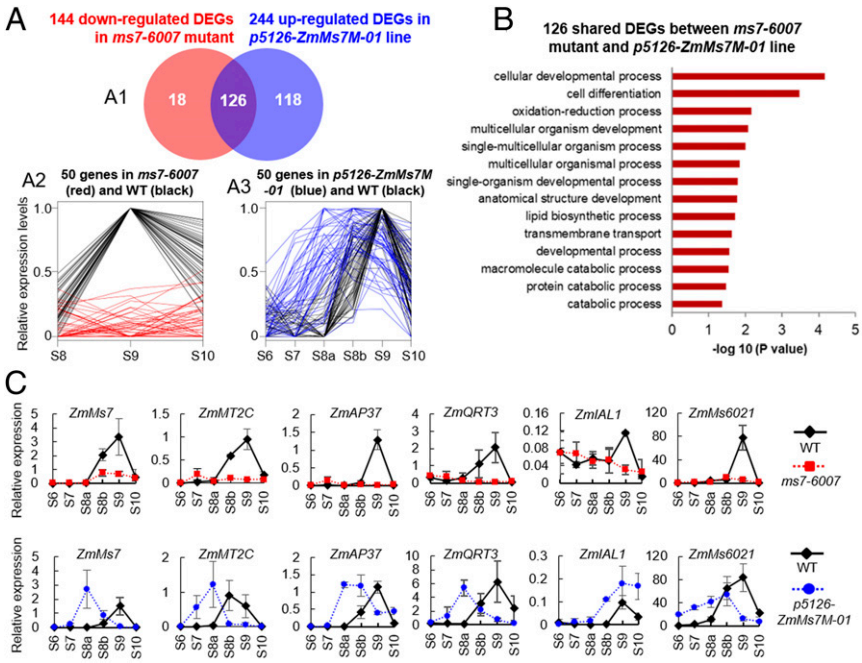

Fig. 6. *p5126* promoter drives premature expression of *ZmMs7*-activated genes and results in the dominant male-sterility phenotype of the *p5126-ZmMs7M-01* line. (*A*) The 126 shared DEGs between 144 down-regulated DEGs in the *ms7-6007* mutant and 244 up-regulated DEGs in the *p5126-ZmMs7M-01* line (A1). The expression patterns of the 50 representative genes in anther transcriptomes of *ms7-6007* mutant at stages 8 to 9 (A2) and in the *p5126-ZmMs7M-01* line at stages 6 to 10 (A3) are shown, respectively. (*B*) Gene ontology enrichment analysis of the 126 shared genes. (*C*) RT-qPCR analysis of *ZmMs7* and five putative activated genes in WT, *ms7-6007*, and the *p5126-ZmMs7M-01* line anthers at stages 6 to 10.

plants, NF-Y subunits interact with various types of transcriptional regulators to form multiple kinds of complexes, thereby regulating individual biological processes (35–38). Here we identified a PHD-type TF as a NF-Y interactor though the domain of ZmMs7 required for association with the NF-Ys need to be further defined. PHD finger proteins are versatile epigenome readers that activate or repress gene expression through recruitments of multiprotein complexes of TFs and chromatin regulators (39). Many PHD finger proteins bind to histone H3 tails with trimethylated lysine 4 (H3K4me3), which is a transcription activation mark (40). We speculate that the fundamental function of ZmMs7 may be recognizing epigenetic marks (e.g., H3K4me3) on its target genes. ZmMs7 may then recruit NF-Y subunits to form multiprotein complexes that activate target gene expression. Notably, we cannot rule out the possibility of ZmMs7 interacting with TFs other than the NF-Y subunits. Logically, ZmMs7 may recruit different interactors when regulating different types of genes. Anyway, elucidating the epigenetic reader role and identifying more interaction partners will help to fully understand the regulatory mechanisms of *ZmMs7* and its homologous genes in plants.

Premature expression of *ZmMs7* in maize driven by *p5126* led to dominant male sterility with completely aborted pollen formation. Unlike most of male-sterility mutants, almost no exine structure was detected on the microspore surface in the *p5126-ZmMs7M-01* line, and instead only irregular deposition of lipid droplets was observed. The severely defective pollen wall is a main feature of the dominant male sterility in the *p5126-ZmMs7M-01* line. A wide range of genes potentially involved in tapetum development and pollen exine formation displayed altered expression patterns in the *p5126-ZmMs7M-01* line. Anther development is a complicated and tightly controlled biological process. Obviously, the disturbance on gene networks responsible for tapetum and pollen development by the *p5126-ZmMs7* element is the molecular basis underlying the dominant male sterility. Given that the regulatory systems by *ZmMs7* and its orthologs are conserved in plants (13, 20, 24, 25), the dominant male sterility of *p5126-ZmMs7* transgenic rice and *Arabidopsis* plants may be caused by similar molecular mechanisms.

Crop heterosis utilization requires preventing self-pollination of the female inbred parents. It is well known that male sterility is the most effective way to ensure cross-pollination and produce pure hybrid seeds (2, 41, 42). The *ZmMs7* gene and its mutant *ms7-6007* have been reported to develop the multi-control sterility system in our laboratory, and the system can be used to maintain and propagate maize recessive male-sterility lines and has several advantages as described (13), e.g., no transgenic element in male-sterility lines and hybrid seeds. Here, we tested genetic stability of the *ms7-6007* male-sterility lines and found that among 403 F_2 populations, 6 (1.5%) type I ($0 \le P$ values < 0.05 and $1.2 <$ ratios ≤ 1.6) and 21 (5.2%) type III ($0 \le P$ values < 0.05 and $7.0 <$ ratios ≤ 42.0) populations showed segregation deviated from the expected 3:1 ratio. For the 21 type III populations with the fertile/sterile ratios far more than 3:1, the reason may be that exogenetic fertile pollen unexpectedly participates in the self-pollination of F_1 plants. The only 1.5% type I F_2 populations showed the fertile/sterile ratios significantly less than 3:1, possibly due to the smaller sample amount of the investigated F_2 individuals (35 to 49 plants) or environmental conditions. Nevertheless, the genotypes of the two types of F_2 individuals completely matched with their corresponding phenotypes (*SI Appendix*, Fig. S9 and Table S3). Therefore, the *ms7-6007* male sterility is fairly stable under different maize genetic backgrounds. In addition, we investigated the effects of *ms7-6007* mutation on grain yield and other agronomic traits in hybrid maize production, and found that *ms7-6007* mutation has no obvious negative effects on maize heterosis and field production. Taken together, based on the developed multi-control sterility system (13), the *ZmMs7* gene and its mutant *ms7-6007* are applicable for hybrid maize breeding and seed production. On the other hand, we developed the *p5126-ZmMs7M*-based DMS

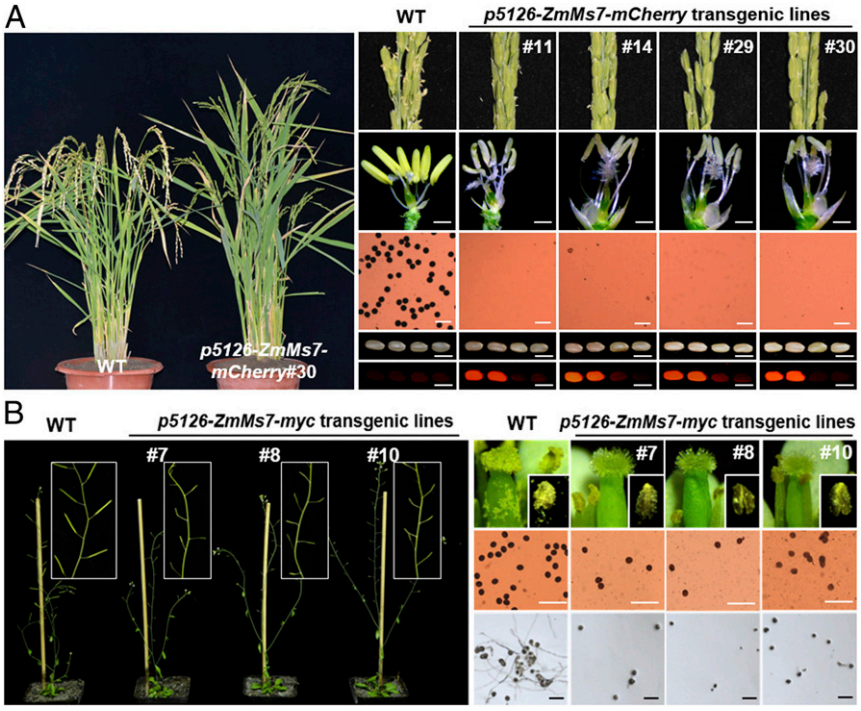

Fig. 7. Dominant male-sterility phenotype of *p5126-ZmMs7* transgenic rice and *Arabidopsis* plants. (*A*) Four rice transgenic plants expressing *p5126-ZmMs7-mCherry* show complete male-sterility phenotypes. Comparison of whole plants after heading, panicles at anthesis, anthers (Scale bars, 1 mm.), pollen grains with I_2-KI staining (Scale bars, 100 μm.), and seeds under bright field and a red fluorescence filter (Scale bars, 0.5 cm.) among WT and four *p5126-ZmMs7* transgenic lines. (*B*) Three *Arabidopsis* plants expressing *p5126-ZmMs7-myc* show complete male sterility of pollen grains. Comparison of siliques, the surface of stigmas and anthers, pollen grains stained with I_2-KI and pollen germination among WT and three transgenic lines. (Scale bars, 100 μm.) The numbers in *A* and *B* indicate different independent transgenic events.

system to create dominant male-sterility lines in maize and rice and found that genetic stability of the *p5126-ZmMs7M* male-sterility lines is relatively high under different maize genetic backgrounds (*SI Appendix*, Fig. S15 and Table S7). Notably, the two different male-sterility systems (multi-control sterility and DMS) are developed by using the same gene *ZmMs7* with different maize promoters and molecular mechanisms underlying male sterility. For the multi-control sterility system, loss of function of *ZmMs7* that encodes a transcriptional activator inactivates its regulated downstream genes related to cutin biosynthesis and tapetal cell PCD, thus causing the delayed tapetal degeneration, abnormal Ubisch body development, and pollen wall formation, and ultimately leads to complete male sterility of the *ms7-6007* mutant. Only plants with the homozygous mutation genotype (*ms7-6007*/*ms7-6007*) display complete male-sterility phenotypes, and thus are named as recessive male-sterility lines. However, for the DMS system, premature expression of *ZmMs7* driven by *p5126* induces the altered expression patterns (i.e., early and high expressions) of a wide range of genes potentially involved in tapetum development and pollen exine formation, and thus results in complete male sterility of the *p5126-ZmMs7M* lines. Plants with the hemizygous genotype (*p5126-ZmMs7M*/-//*ZmMs7*/*ZmMs7*) show complete male-sterility phenotypes but female fertility and normal vegetative growth, and thus are named as dominant male-sterility lines.

The DMS system produces two types of F_1 hybrid seeds, i.e., the red fluorescent transgenic dominant male-sterility seeds (DMS hybrid seeds) and normal color nontransgenic male-fertility seeds (*SI Appendix*, Fig. S13*C*). For cross-pollinated plants such as maize, sunflower, and *Brassica campestris* L., the two types of F_1 hybrid seeds can be flexibly used for crop field production in different countries. For example, in some countries where planting transgenic crops is prohibited, the nontransgenic male-fertility hybrid seeds can be sorted out and planted in the field, while in other countries where transgenic crops are allowed to grow, both of the two types of F_1 hybrid seeds can be mixed up and planted. Although 50% DMS transgenic dominant male-sterility F_1 plants are male sterile, the other 50% nontransgenic male-fertility F_1 sibling plants can provide enough pollen grains to pollinate the male sterile F_1 plants and ensure no impact on the field yield as reported previously (17). On the other hand, for self-pollinated plants such as rice, sorghum, and millet, the nearly 50% nontransgenic male-fertility hybrid seeds can be sorted out and grown in the field. Compared with the CMS and other biotechnology-based male-sterility systems, the DMS system has several potential advantages. First, relative to the CMS system, the DMS lines are created by using premature expression of a single gene *ZmMs7* and show the high stability of male sterility under different genetic backgrounds. Second, compared with the seed production technology and multi-control sterility systems (12–14), the DMS system is not limited by the lack of GMS mutants and fertility restorer genes in many crops. Third, compared with the Barnase/Barstar system (2, 43, 44), the DMS system utilizes a plant endogenous gene (*ZmMs7*) and promoter (*p5126*) to generate male sterile lines, which has no ethical problems. Together, the DMS system is a simple, cost-effective, and multiple-crop applicable biotechnology.

Materials and Methods

The *ms7-6007* mutant (No. 712AA) was sourced from the Maize Genetics Cooperation Stock Center (maizecoop.cropsci.illinois.edu). Methodological details of plant growth, male-sterility stability analysis, cytological observation, RNA-seq, lipidomic analysis, gene expression analysis, dual-luciferase assay, subcellular localization, protein-protein interaction, and protein-DNA interaction assays are described in *SI Appendix*, *Supplemental Materials and Methods*. The primers used in this study are listed in *SI Appendix*, Table S8.

Data Availability. A complete set of RNA-seq raw data has been deposited in the National Center for Biotechnology Information (NCBI) Gene Expression Omnibus (GEO) database (accession no. PRJNA637676). RNA-seq data in *ms7-6007* and WT anther transcriptomes as well as *p5126-ZmMs7M-01* and WT anther transcriptomes are listed in *SI Appendix*, Tables S1, S5, and S6. Genotypic data of 3,072 SNP markers in 403 and 392 maize inbred lines used for male-sterility stability analysis of *ms7-6007* and *p5126-ZmMs7M-01*, respectively, are listed in *SI Appendix*, Tables S3 and S7. Lipidomic data of WT and *ms7-6007* anthers are listed in *SI Appendix*, Table S2. Phenotypic data of the investigated 17 agronomic traits for testing the effects of the *ms7-6007* mutation on maize heterosis and field production are listed in *SI Appendix*, Table S4.

ACKNOWLEDGMENTS. The National Key Research and Development Program of China (2018YFD0100806, 2017YFD0100304, 2017YFD0102001, and 2017YFD0101201), the National Natural Science Foundation of China (31900610, 31971958, 31771875, and 31871702), the Fundamental Research Funds for the Central Universities of China (06500136), and the Beijing Science and Technology Plan Program (Z191100004019005) supported this work.

1. M. Tester, P. Langridge, Breeding technologies to increase crop production in a changing world. *Science* **327**, 818–822 (2010).
2. X. Wan *et al*., Maize genic male-sterility genes and their applications in hybrid breeding: Progress and perspectives. *Mol. Plant* **12**, 321–342 (2019).
3. L. Chen, Y.-G. Liu, Male sterility and fertility restoration in crops. *Annu. Rev. Plant Biol.* **65**, 579–606 (2014).
4. Y.-J. Kim, D. Zhang, Molecular control of male fertility for crop hybrid breeding. *Trends Plant Sci.* **23**, 53–65 (2018).
5. S. H. Cheng, J. Y. Zhuang, Y. Y. Fan, J. H. Du, L. Y. Cao, Progress in research and development on hybrid rice: A super-domesticate in China. *Ann. Bot.* **100**, 959–966 (2007).
6. J.-Z. Huang, Z. G. E, H. L. Zhang, Q. Y. Shu, Workable male sterility systems for hybrid rice: Genetics, biochemistry, molecular biology, and utilization. *Rice (N. Y.)* **7**, 13 (2014).
7. M.-E. Williams, Genetic engineering for pollination control. *Trends Biotechnol.* **13**, 344–349 (1995).
8. L. Yuan, Purification and production of foundation seed of rice PGMS and TGMS lines. *Hybrid Rice* **6**, 1–3 (1994).
9. Z.-A. Wilson, D. B. Zhang, From *Arabidopsis* to rice: Pathways in pollen development. *J. Exp. Bot.* **60**, 1479–1492 (2009).
10. J. Shi, M. Cui, L. Yang, Y. J. Kim, D. Zhang, Genetic and biochemical mechanisms of pollen wall development. *Trends Plant Sci.* **20**, 741–753 (2015).
11. X. Wan, S. Wu, Z. Li, X. An, Y. Tian, Lipid metabolism: Critical roles in male fertility and other aspects of reproductive development in plants. *Mol. Plant* **13**, 955–983 (2020).
12. Y. Wu *et al*., Development of a novel recessive genetic male sterility system for hybrid seed production in maize and other cross-pollinating crops. *Plant Biotechnol. J.* **14**, 1046–1054 (2016).
13. D. Zhang *et al*., Construction of a multicontrol sterility system for a maize male-sterile line and hybrid seed production based on the *ZmMs7* gene encoding a PHD-finger transcription factor. *Plant Biotechnol. J.* **16**, 459–471 (2018).
14. X. An *et al*., *ZmMs30* encoding a novel GDSL lipase is essential for male fertility and valuable for hybrid breeding in maize. *Mol. Plant* **12**, 343–359 (2019).
15. T. Zhu *et al*., Genome-wide analysis of maize GPAT gene family and cytological characterization and breeding application of *ZmMs33/ZmGPAT6* gene. *Theor. Appl. Genet.* **132**, 2137–2154 (2019).
16. Z. Chang *et al*., Construction of a male sterility system for hybrid rice breeding and seed production using a nuclear male sterility gene. *Proc. Natl. Acad. Sci. U.S.A.* **113**, 14145–14150 (2016).
17. T. Fox *et al*., A single point mutation in *Ms44* results in dominant male sterility and improves nitrogen use efficiency in maize. *Plant Biotechnol. J.* **15**, 942–952 (2017).
18. H. Wang, X. W. Deng, Development of the "third-generation" hybrid rice in China. *Genomics Proteomics Bioinformatics* **16**, 393–396 (2018).
19. Z.-A. Wilson, S. M. Morroll, J. Dawson, R. Swarup, P. J. Tighe, The *Arabidopsis MALE STERILITY1* (*MS1*) gene is a transcriptional regulator of male gametogenesis, with homology to the PHD-finger family of transcription factors. *Plant J.* **28**, 27–39 (2001).
20. T. Ito *et al*., *Arabidopsis* MALE STERILITY1 encodes a PHD-type transcription factor and regulates pollen and tapetum development. *Plant Cell* **19**, 3549–3562 (2007).
21. T. Ito, K. Shinozaki, The *MALE STERILITY1* gene of *Arabidopsis*, encoding a nuclear protein with a PHD-finger motif, is expressed in tapetal cells and is required for pollen maturation. *Plant Cell Physiol.* **43**, 1285–1292 (2002).
22. C. Yang, G. Vizcay-Barrena, K. Conner, Z. A. Wilson, MALE STERILITY1 is required for tapetal development and pollen wall biosynthesis. *Plant Cell* **19**, 3530–3548 (2007).
23. Z. Yang *et al*., *OsMS1* functions as a transcriptional activator to regulate programmed tapetum development and pollen exine formation in rice. *Plant Mol. Biol.* **99**, 175–191 (2019).
24. H. Li *et al*., PERSISTENT TAPETAL CELL1 encodes a PHD-finger protein that is required for tapetal cell death and pollen development in rice. *Plant Physiol.* **156**, 615–630 (2011).
25. J. Fernández Gómez, Z. A. Wilson, A barley PHD finger transcription factor that confers male sterility by affecting tapetal development. *Plant Biotechnol. J.* **12**, 765–777 (2014).
26. G. Vizcay-Barrena, Z. A. Wilson, Altered tapetal PCD and pollen wall development in the *Arabidopsis ms1* mutant. *J. Exp. Bot.* **57**, 2709–2717 (2006).
27. K. Hiratsu, K. Matsui, T. Koyama, M. Ohme-Takagi, Dominant repression of target genes by chimeric repressors that include the EAR motif, a repression domain, in *Arabidopsis*. *Plant J.* **34**, 733–739 (2003).
28. A.-M. Cigan *et al*., Phenotypic complementation of *ms45* maize requires tapetal expression of MS45. *Sex. Plant Reprod.* **14**, 135–142 (2001).
29. M.-M. Evans, The indeterminate gametophyte1 gene of maize encodes a LOB domain protein required for embryo Sac and leaf development. *Plant Cell* **19**, 46–62 (2007).
30. G.-L. Nan *et al*., MS23, a master basic helix-loop-helix factor, regulates the specification and development of the tapetum in maize. *Development* **144**, 163–172 (2017).
31. J. Yi *et al*., Defective tapetum cell death 1 (DTC1) regulates ROS Levels by binding to metallothionein during tapetum degeneration. *Plant Physiol.* **170**, 1611–1623 (2016).
32. N. Niu *et al*., EAT1 promotes tapetal cell death by regulating aspartic proteases during male reproductive development in rice. *Nat. Commun.* **4**, 1445 (2013).
33. Z.-A. Myers, B.-F. Holt 3rd, NUCLEAR FACTOR-Y: Still complex after all these years? *Curr. Opin. Plant Biol.* **45**, 96–102 (2018).
34. Z. Zhang, X. Li, C. Zhang, H. Zou, Z. Wu, Isolation, structural analysis, and expression characteristics of the maize nuclear factor Y gene families. *Biochem. Biophys. Res. Commun.* **478**, 752–758 (2016).
35. H. Zhao *et al*., The *Arabidopsis thaliana* nuclear factor Y transcription factors. *Front Plant Sci* **7**, 2045 (2017).
36. S. Das, S. K. Parida, P. Agarwal, A. K. Tyagi, Transcription factor OsNF-YB9 regulates reproductive growth and development in rice. *Planta* **250**, 1849–1865 (2019).
37. K. Hwang, H. Susila, Z. Nasim, J. Y. Jung, J. H. Ahn, *Arabidopsis* ABF3 and ABF4 transcription factors Act with the NF-YC complex to regulate SOC1 expression and mediate drought-accelerated flowering. *Mol. Plant* **12**, 489–505 (2019).
38. B. K. Bello *et al*., NF-YB1-YC12-bHLH144 complex directly activates *Wx* to regulate grain quality in rice (*Oryza sativa* L.). *Plant Biotechnol. J.* **17**, 1222–1235 (2019).
39. R. Sanchez, M.-M. Zhou, The PHD finger: A versatile epigenome reader. *Trends Biochem. Sci.* **36**, 364–372 (2011).
40. J. Gatchalian, "PHD fingers as histone readers" in *Histone Recognition*, Z.-Z. Zhou, Ed. (Springer, 2015), pp. 27–47.
41. E. Perez-Prat, M. M. van Lookeren Campagne, Hybrid seed production and the challenge of propagating male-sterile plants. *Trends Plant Sci.* **7**, 199–203 (2002).
42. K. Kempe, M. Gils, Pollination control technologies for hybrid breeding. *Mol. Breed.* **27**, 417–437 (2011).
43. C. Mariani *et al*., Induction of male sterility in plants by a chimaeric ribonuclease gene. *Nature* **347**, 737–741 (1990).
44. C. Mariani *et al*., A chimaeric ribonuclease-inhibitor gene restores fertility to male sterile plants. *Nature* **357**, 384–387 (1992).